the $-CH_2-$ protons of the bridging dppm ligands at δ +4.15 (±0.02), with associated P–H coupling, and only a single resonance for the methyl groups (δ +2.06) of the acetonitrile ligands, and one triplet (δ +0.63) and one quartet (δ +2.31) for the ethyl groups of the propionitrile complex. The $^{31}P\{^1H\}$ NMR spectra (recorded in CD_2Cl_2/CH_2Cl_2) reveal an apparent singlet for all three bis-nitrile salts (δ −17.9 to −18.6). These data taken in conjunction with IR spectral evidence for a bridging CO ligand support a structure in which the pair of RCN ligands are co-planar with the Re(μ-CO)Re unit and either both cis or both trans to it (see structures IV and V). The similarity of the electrochemical properties of these complexes to those of the *all-cis* isomers $[Re_2Cl_3(dppm)_2(CO)_2(NCR)]PF_6$ favors structure IV as the most likely possibility of the two.

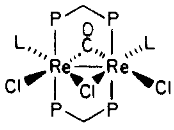
IV

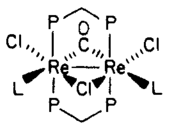
V

(L = RCN)

(f) Concluding Remarks. As we have now demonstrated, the triply bonded complexes $Re_2X_4(dppm)_2$ (X = Cl or Br) have a very rich chemistry. They react readily with CO, without bond cleavage, to give monocarbonyls and, in the case of X = Cl, a dicarbonyl complex.[19] The monocarbonyls are rare examples of multiply bonded A-frame-like molecules. A more detailed appraisal of the electronic structures and metal–metal bond orders of $Re_2X_4(dppm)_2(CO)$ and the related monoisocyanide complexes remains for future consideration.[15,24]

The reactions of the monocarbonyl complex $Re_2Cl_4(dppm)_2(CO)$ with isocyanide ligands are of special interest since we see here examples of rarely encountered structural isomerization in multiply bonded edge-shared bioctahedral complexes. In the case of the aryl isocyanides xylylNC and mesitylNC, we obtained the complexes $Re_2(\mu\text{-}Cl)(\mu\text{-}CO)(\mu\text{-}dppm)_2Cl_3(CNR)$ which bear a very close structural relationship to the related dicarbonyl complex $Re_2(\mu\text{-}Cl)(\mu\text{-}CO)(\mu\text{-}dppm)_2Cl_3(CO)$. The less effective π-acceptor alkyl isocyanide ligands *i*-PrNC and *t*-BuNC favor the alternative di-μ-chloro structure $Re_2(\mu\text{-}Cl)_2(\mu\text{-}dppm)_2Cl_2(CO)(CNR)$. This structural difference is accompanied by a significant change in the nature of the metal-based HOMO as judged by cyclic voltammetric electrochemical measurements.

Acknowledgment. Support from the National Science Foundation (Grant No. 85-06702 to R.A.W. and Grant No. 8211407 to F.A.C.) is gratefully acknowledged. We thank William S. Harwood and Stephen M. Tetrick for assistance with some of the NMR spectral studies.

Registry No. 1, 96306-83-1; **2**, 102781-91-9; $Re_2Br_4(dppm)_2(CO)$, 102781-92-0; $Re_2Br_4(dppm)_2$, 58312-72-4; $Re_2Cl_4(dppm)_2(CO)(CNCHMe_2)$, 102781-93-1; $Re_2Cl_4(dppm)_2(CO)(CNCMe_3)$, 102781-94-2; $Re_2Cl_4(dppm)_2(CO)(CNmesityl)$, 102781-95-3; $[Re_2Cl_3(dppm)_2(CO)(NCCH_3)_2]PF_6$, 102781-97-5; $[Re_2Cl_3(dppm)_2(CO)(NCC_2H_5)_2]PF_6$, 102781-99-7; $[Re_2Cl_3(dppm)_2(CO)(NCC_6H_5)_2]PF_6$, 102782-01-4; Re, 7440-15-5.

Supplementary Material Available: Tables of anisotropic displacement parameters, full lists of bond lengths and angles, and observed and calculated structure factors for $Re_2Cl_4(dppm)_2(CO)$ (**1**) and $Re_2Cl_4(dppm)_2(CO)(CNxylyl)$ (**2**) (33 pages). Ordering information is given on any current masthead page.

The Multiply Bonded Octahalodiosmate(III) Anions. 2.[1] Structure and Bonding

Pradyot A. Agaskar,[2a] F. Albert Cotton,*[2a] Kim R. Dunbar,[2a] Larry R. Falvello,[2a] Stephen M. Tetrick,[2b] and Richard A. Walton*[2b]

Contribution from the Department of Chemistry and Laboratory for Molecular Structure and Bonding, Texas A&M University, College Station, Texas 77843, and Department of Chemistry, Purdue University, West Lafayette, Indiana 47907. *Received January 17, 1986*

Abstract: The green crystalline compounds $[(n\text{-}Bu)_4N]_2[Os_2X_8]$ (X = Cl (**1**), Br (**2**)) have been prepared, and their crystal and electronic structures have been studied. The two compounds form isotypic crystals in space group $P\bar{1}$, with the following unit cell dimensions, given first for **1** and then for **2**: a = 11.797 (2), 12.143 (3) Å; b = 18.650 (4), 18.687 (6) Å; c = 11.506 (2), 11.764 (3) Å; α = 104.73 (1)°, 103.58 (2)°; β = 103.06 (1)°, 105.06 (2)°; γ = 100.00 (1)°, 99.81 (2)°; V = 2312 (2), 2428 (1) Å^3. With Z = 2, the molecular formula defines the asymmetric unit and no crystallographic symmetry is imposed on the $Os_2X_8^{2-}$ ions. In fact, they come very close to having D_{4d} symmetry, with the following dimensions for **1** and **2**: Os–Os, 2.182 (1), 2.196 (1) Å; Os–X(av), 2.322 [6], 2.444 [4] Å; ∠Os–Os–X, 104.2 (3)°, 104.3 (4)°; mean torsion angle, 49.0 [3]°, 46.7 [1]°. The electronic structure of the $Os_2Cl_8^{2-}$ ion in its eclisped (D_{4h}) conformation has been calculated by the SCF-Xα–SW method, including relativistic corrections. The results support the shorthand description of the metal–metal bond as a d^5–d^5, $\sigma^2\pi^4\delta^2\delta^{*2}$, triple bond. The HOMO is the $2b_{1u}$ (δ^*) orbital, followed closely (~0.3 eV) by the $2b_{2g}$ (δ) orbital. The Os–Os π bonding is concentrated mainly in the $2e_u$ orbital and the σ bonding almost entirely in the $2a_{1g}$ orbital. Both of these are very stable, thus accounting for the shortness of the Os–Os bond.

The $Re_2Cl_8^{2-}$ ion is the archetypal species in the field of multiple bonds between metal atoms.[3-5] It owes this distinction not only to the historical fact that it provided the first recognized example of a quadruple bond[3] but also because the M_2X_8 structure is a

---

(1) Part 1: Fanwick, P. E.; King, M. K.; Tetrick, S. M.; Walton, R. A. *J. Am. Chem. Soc.* **1985**, *107*, 5009.

(2) (a) Texas A&M University. (b) Purdue University.

(3) Cotton, F. A.; Johnson, B. F. G.; Robinson, W. R. *Inorg. Chem.* **1965**, *4*, 326.

(4) (a) Cotton, F. A.; Walton, R. A. *Multiple Bonds Between Metal Atoms*; John Wiley & Sons: New York, 1982. (b) Cotton, F. A.; Walton, R. A. *Struct. Bonding (Berlin)* **1985**, *62*, 1.

(5) Cotton, F. A.; Mott, G. N.; Schrock, R. R.; Sturgeoff, L. G. *J. Am. Chem. Soc.* **1982**, *104*, 6781.

0002-7863/86/1508-4850$01.50/0

Table I. Crystal Data for $(n\text{-}Bu_4N)_2[Os_2Cl_8]$ (**1**) and $(n\text{-}Bu_4N)_2[Os_2Br_8]$ (**2**)

formula	$Os_2Cl_8N_2C_{32}H_{72}$ (**1**)	$Os_2Br_8N_2C_{32}H_{72}$ (**2**)
formula wt	1149.0	1504.6
space group	$P\bar{1}$	$P\bar{1}$
systematic absences	none	none
a, Å	11.797 (2)	12.143 (3)
b, Å	18.650 (4)	18.687 (6)
c, Å	11.506 (2)	11.764 (3)
α, deg	104.73 (1)	103.58 (2)
β, deg	103.06 (1)	105.06 (2)
γ, deg	100.00 (1)	99.81 (2)
V, Å^3	2312 (2)	2428 (1)
Z	2	2
d_{calcd}, g/cm^3	1.65	2.06
crystal size, mm	0.30 × 0.12 × 0.09	0.69 × 0.18 × 0.16
μ(Mo Kα), cm^{-1}	63.0	125
data collection instrument	Enraf-Nonius CAD-4F	Syntex P$\bar{1}$
radiation (monochromated in incident beam)	Mo Kα ($\lambda_{\bar{\alpha}}$ = 0.71073 Å)	Mo Kα ($\lambda_{\bar{\alpha}}$ = 0.71073 Å)
orientation reflectns, no., range (2θ)	25; 10–29°	15; 22–30°
temp, °C	27 ± 4	14 ± 6
scan method	ω–2θ	ω–2θ
data col. range, 2θ, deg	4.0–50.0	4.0–48.0
no. of unique data, total	6420	6446
with $F_o^2 > 3\sigma(F_o^2)$	5157	4735
no. of parameters refined	377	360
trans. factors, max, min	1.00, 0.82	1.00, 0.61
R^a	0.0475	0.0426
R_w^b	0.0652	0.0568
quality-of-fit indicator^c	1.673	1.099
largest shift/esd, final cycle	0.55	0.47
largest peak, e/Å^3	1.22	0.93

[a] $R = \sum||F_o| - |F_c||/\sum|F_o|$. [b] $R_w = [\sum w(|F_o| - |F_c|)^2/\sum w|F_o|^2]^{1/2}$; $w = 1/\sigma^2(|F_o|)$. [c] Quality-of-fit $= [\sum w(|F_o| - |F_c|)^2/(N_{obsd} - N_{parameters})]^{1/2}$.

fundamental paradigm upon which much of our understanding[4] of M–M multiple bonds is based. Including the $Re_2Cl_8^{2-}$ ion itself, a complete list of the $M_2X_8^{n-}$ species that have now been prepared and studied to various extents is as follows:

$$Cr_2X_8^{4-}\ (X = CH_3)$$

$$Mo_2X_8^{4-}\ (X = Cl,\ Br,\ NCS,\ CH_3)$$

$$W_2X_8^{4-}\ (X = Cl,\ CH_3)$$

$$Tc_2X_8^{2-}\ (X = Cl,\ Br)$$

$$Tc_2X_8^{3-}\ (X = Cl)$$

$$Re_2X_8^{2-}\ (X = Cl,\ Br,\ I,\ NCS,\ NCSe,\ CH_3)$$

$$Os_2X_8^{2-}\ (X = Cl,\ Br)$$

It is with the last two species in the above list that this report is concerned. Our recent synthesis of salts of the multiply bonded octahalodiosmate(III) anions $Os_2X_8^{2-}$ (X = Cl or Br) has provided for the first time examples of homoleptic halide anions of this type for one of the platinum metals.[1] Furthermore, these species constitute the first examples of metal–metal triply bonded halide anions $M_2X_8^{n-}$ for any of the transition elements.[4] The structure of the $Os_2Cl_8^{2-}$ ion has been briefly described, as its $Ph_3PNPPh_3^+$ salt, in a recent preliminary communication,[1] but this compound unfortunately displayed considerable crystallographic disorder. The $N(n\text{-}C_4H_9)_4^+$ salts of both $Os_2Cl_8^{2-}$ and $Os_2Br_8^{2-}$, which are described here, are much more amenable to clean crystallographic characterization. In addition, we present the results of an SCF–Xα–SW calculation for the $Os_2Cl_8^{2-}$ ion which provides a basis for discussing its electronic structure.

Experimental Procedures

Preparations. Synthesis of $(n\text{-}Bu_4N)_2Os_2X_8$ (X = Cl or Br). The generation of solutions that contain the $Os_2X_8^{2-}$ anions was performed as described previously.[1] A sample of the acetate complex $Os_2(O_2CCH_3)_4Cl_2$[6] was suspended in ethanol which had been saturated with gaseous HX (X = Cl or Br). The mixture was refluxed for 1.5 h, and the resulting solution was treated with an ethanol solution that contained an excess of $n\text{-}Bu_4NBr$. The reaction solvent was then evaporated under a stream of gaseous nitrogen until the green crystals of $(n\text{-}Bu_4N)_2Os_2X_8$ had separated. Full details of synthetic procedures and spectroscopic and electrochemical properties of these and other salts of the anions will be presented in a future paper.[7]

Table II. Input Parameters Used for SCF–Xα–SW Calculation on $Os_2Cl_8^{2-}$

atom	sphere radius, Å	α value
outer sphere	4.0942	0.71864
Os	1.3332	0.69280
Cl	1.3823	0.72325

Preparations of Single Crystals of $(n\text{-}Bu_4N)_2Os_2X_8$. Crystals were grown under a nitrogen atmosphere, and all solvents were thoroughly deoxygenated before use. A sample of $(n\text{-}Bu_4N)_2Os_2Cl_8$ (100 mg) was dissolved in CH_2Cl_2 (5 mL) and filtered into a 3-dram sample vial. Toluene (5 mL) was carefully layered on top of this solution, and the vial was then capped. After 1 week the solvent mixture was decanted off and the crystals were washed very carefully with ethanol and ether. Crystals of $(n\text{-}Bu_4N)_2Os_2Br_8$ were grown from CH_2Cl_2/toluene in a manner identical with that described for the chloride.

X-ray Crystallography. Crystals of $(n\text{-}Bu_4N)_2[Os_2Cl_8]$ (**1**) and $(n\text{-}Bu_4N)_2[Os_2Br_8]$ (**2**), both green and acicular, were mounted at the ends of glass fibers and covered with epoxy cement. Geometric and intensity data for compounds **1** and **2** were taken by automated diffractometers (Enraf-Nonius CAD-4F and Syntex P$\bar{1}$, respectively) by following procedures described previously.[8] The unit cell parameters of **1** and **2**, given in Table I along with other crystal data, were found to be similar; both are triclinic. Axial photography was used to verify the lattice dimensions, and least-squares analysis was used to refine the cell dimensions and the orientation matrix for each of the crystals.

Intensity data for the crystals of **1** and **2**, gathered by the ω–2θ scan technique, were reduced by routine procedures.[9] Absorption corrections were applied to both data sets,[10] based on azimuthal scans of several reflections with diffractometer angle χ near 90°. After equivalent data had been averaged, there remained 5157 data for compound **1** and 4735 for compound **2**, with $F_o^2 \geq 3\sigma(F_o^2)$; these were used in the subsequent development and refinement of the structures.

The two unique osmium atoms in each structure were located via Patterson maps; the coordinates of atoms in the $Os_2X_8^{2-}$ units were quite similar in the two cases. The structure of compound **1** was developed routinely in an alternating sequence of least-squares refinements and difference Fourier maps. The crystallographic asymmetric unit was found to consist of one formula unit of $(n\text{-}Bu_4N)_2[Os_2Cl_8]$. In the final least-squares refinement, four carbon atoms on n-butyl groups were refined isotropically because of poor behavior of their anisotropic displacement parameters in earlier cycles. All other atoms were refined anisotropically, giving a data:parameter ratio of 13.7. The refinement converged to the figures of merit given in Table I. A difference Fourier map following the refinement had three peaks above 1 e/Å^3, all of which were ghosts of existing atoms.

The structure of **2** was also developed and refined in a series of least-squares refinements and difference Fourier maps. The asymmetric unit was found to consist of one formula unit of $(n\text{-}Bu_4N)_2[Os_2Br_8]$. The atoms of the $Os_2Br_8^{2-}$ moiety refined quite steadily, but several atoms of the n-butyl groups gave minor difficulties. There was significant, though not serious, correlation among the parameters of these groups. For C(17), displacement parameters continued to oscillate by ca. 1σ late in refinement; these parameters were therefore fixed in the final cycle. None of the features observed for the butyl groups is surprising, in view of the fact that the 10 atoms of the complex anion possess ~61% of the scattering power of the asymmetric unit, while the remaining 34 atoms have only ~39%. There is also an indication that the structure of **2** is

---

(6) Behling, T.; Wilkinson, G.; Stephenson, T. A.; Tocher, D. A.; Walkinshaw, M. D. *J. Chem. Soc., Dalton Trans.* **1983**, 2109.

(7) Fanwick, P. E.; Tetrick, S. M.; Walton, R. A., manuscript in preparation.

(8) (a) CAD-4F: Bino, A.; Cotton, F. A.; Fanwick, P. E. *Inorg. Chem.* **1979**, *18*, 3558. (b) Syntex P$\bar{1}$: Cotton, F. A.; Frenz, B. A.; Deganello, G.; Shaver, A. *J. Organomet. Chem.* **1973**, *50*, 227.

(9) Crystallographic computing was done on a PDP-11/60 (RSX-11M V4.1) with PDP-11 simulated VAXSDP, on a VAX-11/780 (VMS V4.1) with VAXSDP, and on a VAX 8600 (VMS V4.1) with VAXSDP.

(10) North, A. C. T.; Phillips, D. C.; Mathews, F. S. *Acta Crystallogr., Sect. A: Cryst. Phys., Diffr., Theor. Crystallogr.* **1968**, *24*, 351.

Table III. Atomic Positional Parameters and Equivalent Isotropic Displacement Parameters (Å^2) and Their Estimated Standard Deviations for $(n\text{-Bu}_4\text{N})_2[\text{Os}_2\text{Cl}_8]$ (**1**)[a]

atom	x	y	z	B(Å^2)
Os(1)	0.45903 (4)	0.31051 (3)	0.17568 (5)	4.31 (1)
Os(2)	0.36104 (4)	0.20257 (3)	0.03188 (4)	3.85 (1)
Cl(1)	0.3134 (3)	0.3587 (2)	0.2540 (3)	6.22 (9)
Cl(2)	0.5158 (4)	0.2753 (2)	0.3567 (3)	6.3 (1)
Cl(3)	0.6542 (3)	0.3222 (3)	0.1706 (4)	7.1 (1)
Cl(4)	0.4537 (4)	0.4019 (2)	0.0719 (3)	6.3 (1)
Cl(5)	0.2004 (3)	0.2319 (2)	−0.0881 (3)	5.27 (8)
Cl(6)	0.2263 (3)	0.1483 (2)	0.1260 (3)	4.84 (7)
Cl(7)	0.4725 (3)	0.1157 (2)	0.0748 (3)	5.16 (7)
Cl(8)	0.4457 (3)	0.2035 (2)	−0.1310 (3)	4.99 (8)
N(1)	0.8101 (8)	0.1226 (6)	−0.0777 (9)	4.9 (3)
N(2)	0.689 (1)	0.6193 (6)	0.3428 (9)	5.0 (3)
C(1)	0.829 (1)	0.2033 (7)	0.012 (1)	5.1 (3)
C(2)	0.958 (1)	0.2393 (9)	0.085 (2)	7.7 (5)
C(3)	0.964 (1)	0.321 (1)	0.181 (1)	10.1 (6)
C(4)	0.946 (2)	0.298 (1)	0.293 (2)	12.1 (8)
C(5)	0.861 (1)	0.0687 (8)	−0.009 (1)	5.3 (4)
C(6)	0.809 (1)	0.0612 (9)	0.101 (1)	6.3 (4)
C(7)	0.892 (2)	0.019 (1)	0.169 (1)	8.5 (5)
C(8)	0.849 (2)	0.006 (1)	0.276 (2)	9.9 (6)
C(9)	0.673 (1)	0.0932 (8)	−0.138 (1)	5.3 (4)
C(10)	0.635 (1)	0.0188 (7)	−0.243 (1)	5.0 (3)
C(11)	0.495 (1)	−0.0008 (9)	−0.292 (1)	6.7 (4)
C(12)	0.451 (2)	−0.076 (1)	−0.399 (2)	8.3 (5)
C(13)	0.879 (1)	0.1255 (8)	−0.172 (1)	5.3 (3)
C(14)	0.842 (1)	0.1756 (9)	−0.256 (1)	6.3 (4)
C(15)	0.906 (2)	0.164 (1)	−0.354 (1)	7.9 (5)
C(16)	0.887 (2)	0.219 (1)	−0.437 (2)	9.0 (6)
C(17)	0.670 (2)	0.550 (1)	0.391 (2)	9.3 (6)
C(18)	0.781 (2)	0.537 (1)	0.463 (2)	8.6 (5)
C(19)	0.755 (2)	0.472 (1)	0.520 (2)	10.6 (7)
C(20)	0.857 (2)	0.448 (2)	0.572 (2)	13.6 (8)*
C(21)	0.782 (2)	0.615 (1)	0.269 (1)	9.1 (6)
C(22)	0.768 (2)	0.551 (1)	0.174 (2)	11.4 (8)
C(23)	0.876 (2)	0.542 (2)	0.117 (2)	16 (1)
C(24)	0.918 (2)	0.590 (2)	0.070 (2)	13.9 (9)*
C(25)	0.570 (1)	0.614 (1)	0.247 (2)	7.7 (5)
C(26)	0.476 (2)	0.626 (1)	0.305 (3)	13.9 (9)
C(27)	0.356 (3)	0.607 (2)	0.211 (3)	15 (1)*
C(28)	0.295 (3)	0.655 (2)	0.188 (3)	18 (1)*
C(29)	0.730 (2)	0.692 (1)	0.452 (2)	8.6 (6)
C(30)	0.742 (2)	0.764 (1)	0.423 (2)	9.7 (6)
C(31)	0.787 (2)	0.833 (1)	0.539 (2)	10.0 (7)
C(32)	0.787 (3)	0.903 (1)	0.514 (3)	13.2 (9)

[a] Starred atoms were refined isotropically. Anisotropically refined atoms are given in the form of the equivalent isotropic displacement parameter defined as $4/3[a^2\beta_{11} + b^2\beta_{22} + c^2\beta_{33} + ab(\cos\gamma)\beta_{12} + ac(\cos\beta)\beta_{13} + bc(\cos\alpha)\beta_{23}]$.

Table IV. Atomic Positional Parameters and Equivalent Isotropic Displacement Parameters (Å^2) and Their Estimated Standard Deviations for $(n\text{-Bu}_4\text{N})_2[\text{Os}_2\text{Br}_8]$ (**2**)[a]

atom	x	y	z	B (Å^2)
Os(1)	0.47274 (4)	0.31325 (3)	0.17516 (5)	3.94 (1)
Os(2)	0.37175 (4)	0.20577 (3)	0.03446 (4)	3.52 (1)
Br(1)	0.3276 (1)	0.36729 (9)	0.2525 (2)	6.66 (4)
Br(2)	0.5286 (2)	0.2771 (1)	0.3652 (1)	6.92 (5)
Br(3)	0.6740 (1)	0.3213 (1)	0.1743 (2)	7.78 (6)
Br(4)	0.4721 (2)	0.40835 (9)	0.0637 (2)	6.67 (5)
Br(5)	0.2026 (1)	0.23691 (9)	−0.0911 (1)	5.53 (4)
Br(6)	0.2370 (1)	0.15034 (8)	0.1329 (1)	5.31 (4)
Br(7)	0.4856 (1)	0.11394 (8)	0.0786 (1)	5.52 (4)
Br(8)	0.4525 (1)	0.20597 (8)	−0.1355 (1)	5.26 (4)
N(1)	0.1867 (9)	0.8773 (6)	0.084 (1)	4.9 (3)
N(2)	0.702 (1)	0.6246 (6)	0.3611 (9)	5.0 (3)
C(1)	0.165 (1)	0.7960 (8)	−0.001 (1)	5.6 (4)
C(2)	0.032 (2)	0.760 (1)	−0.073 (2)	9.7 (6)
C(3)	0.024 (1)	0.6909 (9)	−0.181 (2)	7.2 (5)
C(4a)	0.045 (3)	0.715 (2)	−0.285 (3)	8.2 (8)*
C(4b)	0.041 (4)	0.644 (3)	−0.109 (4)	8 (1)*
C(5)	0.142 (1)	0.9332 (8)	0.017 (1)	5.8 (4)
C(6)	0.192 (1)	0.9406 (9)	−0.089 (1)	6.6 (4)
C(7)	0.116 (2)	0.984 (1)	−0.167 (2)	7.6 (5)
C(8)	0.165 (2)	0.996 (1)	−0.272 (2)	10.5 (8)
C(9)	0.323 (1)	0.9033 (8)	0.144 (1)	5.5 (4)
C(10)	0.362 (1)	0.9765 (8)	0.248 (1)	5.2 (4)
C(11)	0.502 (1)	0.9946 (9)	0.299 (1)	5.7 (4)
C(12)	0.549 (2)	1.069 (1)	0.403 (2)	7.4 (5)
C(13)	0.121 (1)	0.8759 (8)	0.180 (1)	5.2 (4)
C(14)	0.154 (1)	0.8258 (9)	0.259 (1)	6.3 (4)
C(15)	0.096 (2)	0.836 (1)	0.362 (2)	7.7 (5)
C(16)	0.121 (2)	0.782 (1)	0.441 (2)	9.3 (6)
C(17)	0.565 (3)	0.607 (1)	0.359 (2)	14[b]
C(18)	0.518 (3)	0.635 (1)	0.278 (2)	16.1 (9)
C(19)	0.367 (2)	0.610 (1)	0.243 (3)	14 (1)
C(20)	0.285 (2)	0.650 (1)	0.207 (2)	14.9 (9)
C(21)	0.737 (2)	0.599 (1)	0.261 (2)	14.1 (6)
C(22)	0.807 (2)	0.578 (1)	0.221 (2)	15.0 (7)
C(23)	0.833 (3)	0.545 (2)	0.104 (3)	16 (1)*
C(24)	0.925 (4)	0.572 (2)	0.087 (4)	24 (2)*
C(25)	0.743 (3)	0.579 (1)	0.442 (2)	21.0 (8)
C(26)	0.771 (2)	0.526 (1)	0.458 (1)	10.5 (6)
C(27)	0.794 (2)	0.485 (2)	0.541 (2)	13.2 (8)*
C(28)	0.857 (3)	0.437 (2)	0.553 (3)	16 (1)*
C(29)	0.747 (2)	0.704 (1)	0.424 (3)	16 (1)
C(30)	0.738 (2)	0.761 (1)	0.477 (4)	19 (2)
C(31)	0.797 (3)	0.841 (2)	0.545 (3)	14.1 (9)*
C(32)	0.791 (3)	0.901 (2)	0.509 (3)	17 (1)*

[a] Starred atoms were refined isotropically. Anisotropically refined atoms are given in the form of the equivalent isotropic displacement parameter defined as $4/3[a^2\beta_{11} + b^2\beta_{22} + c^2\beta_{33} + ab(\cos\gamma)\beta_{12} + ac(\cos\beta)\beta_{13} + bc(\cos\alpha)\beta_{23}]$. [b] The displacement parameters of atom C(17) were not refined in the final least-squares cycle. See text.

not as rigidly packed as that of **1**. The unit cell of the octabromo complex is ~100 Å larger than that of the $\text{Os}_2\text{Cl}_8{}^{2-}$ species. In addition, one of the terminal methyl groups of an $(n\text{-Bu}_4\text{N})^+$ cation in **2** is disordered; no such feature was observed for the crystal of **1**.

In the final refinement of the structure of $(n\text{-Bu}_4\text{N})_2[\text{Os}_2\text{Br}_8]$, 360 variables were fitted to 4735 data, for a data:parameter ratio of 13.2. The refinement converged with the figures of merit shown in Table I.

For both structures, further absorption corrections were applied according to the method of Walker and Stuart[11] upon convergence of isotropic refinement but before beginning the cycles of anisotropic refinement.

The SCF-Xα-SW Calculation. The input structural parameters were based on the early X-ray crystallographic results and differ slightly but not importantly from the final ones. The $\text{Os}_2\text{Cl}_8{}^{2-}$ ion was restricted to D_{4h} symmetry with the following key dimensions: Os–Os = 2.19 Å; Os–Cl = 2.30 Å; Os–Os–Cl = 103°. The calculation was begun by employing the final molecular charge density and potentials obtained in the earlier calculations on the $\text{Re}_2\text{Cl}_8{}^{2-}$ ion.[12,13] Other input parameters are listed in Table II. In addition, a Watson sphere with a charge of 2+ and a radius of 8.73697 au was used. The general approach is described in more detail in ref 12.

For the nonrelativistic calculation, iteration to self-consistency required 17 cycles. Each new iteration employed a 3:1 average of the initial and final potentials from the preceding one; an energy search was conducted after the fifth iteration and after every two iterations subsequently. The largest change in potential during the last iteration was less than 0.001 hartree (0.027 eV). The relativistically corrected calculation was commenced by using the potential from the converged nonrelativistic calculation; 15 iterations achieved convergence to <0.001 hartrees.

Results

Preparation and Chemical Properties. The $\text{Os}_2\text{X}_8{}^{2-}$ ions are obtained from the readily available starting material $\text{Os}_2(\text{O}_2\text{CCH}_3)_4\text{Cl}_2$. Although this compound is not soluble in ethanol, when a suspension of it in ethanol previously saturated with the appropriate HX gas is refluxed, it reacts and dissolves to give a green solution. Upon addition of excess $n\text{-Bu}_4\text{NBr}$ followed by evaporation in a steam of nitrogen, the green crystalline compounds, $(n\text{-Bu}_4\text{N})_2\text{Os}_2\text{X}_8$, are obtained. The $\text{Os}_2\text{X}_8{}^{2-}$ ions have a broad range of reactivity, some facets of which have already been mentioned.[1] A detailed report is in preparation.[7]

---

(11) Walker, N.; Stuart, D. *Acta Crystallogr., Sect. A: Found. Crystallogr.* **1983**, *39*, 158.

(12) Bursten, B. E.; Cotton, F. A.; Fanwick, P. E.; Stanley, G. E. *J. Am. Chem. Soc.* **1983**, *105*, 3082.

(13) These data, which are not given in ref 12, were retrieved from our archives. By starting the computation in this way many cycles of iteration were avoided.

Table V. Selected Distances, Angles, and Torsion Angles and Their Estimated Standard Deviations for $Os_2Cl_8^{2-}$ (**1**) and $Os_2Br_8^{2-}$ (**2**)

	X = Cl	X = Br
	Distances, Å	
Os(1)-Os(2)	2.182 (1)	2.196 (1)
Os(1)-X(1)	2.322 (3)	2.442 (2)
Os(1)-X(2)	2.332 (3)	2.448 (2)
Os(1)-X(3)	2.290 (3)	2.425 (2)
Os(1)-X(4)	2.318 (3)	2.443 (2)
Os(2)-X(5)	2.315 (3)	2.444 (2)
Os(2)-X(6)	2.345 (2)	2.462 (1)
Os(2)-X(7)	2.335 (2)	2.446 (1)
Os(2)-X(8)	2.317 (3)	2.445 (1)
$[Os-X]_{av}$	2.322 [6]	2.444 [4]
	Angles (deg)	
Os(2)-Os(1)-X(1)	104.87 (8)	105.26 (5)
Os(2)-Os(1)-X(2)	103.76 (8)	103.87 (5)
Os(2)-Os(1)-X(3)	104.48 (9)	104.28 (5)
Os(2)-Os(1)-X(4)	104.81 (8)	104.80 (5)
Os(1)-Os(2)-X(5)	104.62 (8)	105.00 (5)
Os(1)-Os(2)-X(6)	102.90 (7)	102.85 (4)
Os(1)-Os(2)-X(7)	104.20 (8)	104.50 (5)
Os(1)-Os(2)-X(8)	103.69 (8)	103.78 (5)
X(1)-Os(1)-X(2)	88.1 (1)	87.00 (7)
X(1)-Os(1)-X(3)	150.6 (1)	150.43 (7)
X(1)-Os(1)-X(4)	84.5 (1)	85.35 (7)
X(2)-Os(1)-X(3)	86.6 (1)	87.09 (7)
X(2)-Os(1)-X(4)	151.4 (1)	151.33 (7)
X(3)-Os(1)-X(4)	86.4 (1)	86.08 (8)
X(5)-Os(2)-X(6)	87.4 (1)	86.96 (5)
X(5)-Os(2)-X(7)	151.2 (1)	150.49 (6)
X(5)-Os(2)-X(8)	85.8 (1)	85.87 (5)
X(6)-Os(2)-X(7)	86.88 (9)	87.36 (5)
X(6)-Os(2)-X(8)	153.4 (1)	153.37 (6)
X(7)-Os(2)-X(8)	86.74 (9)	86.38 (5)
	Torsion Angles (deg)	
X(1)-Os(1)-Os(2)-X(5)	48.2 (1)	46.43 (6)
X(2)-Os(1)-Os(2)-X(6)	49.2 (1)	46.82 (7)
X(3)-Os(1)-Os(2)-X(7)	49.2 (2)	46.75 (7)
X(4)-Os(1)-Os(2)-X(8)	49.2 (2)	46.64 (7)
$[X-Os(1)-Os(2)-X]_{av}$	49.0 [3]	46.7 [1]

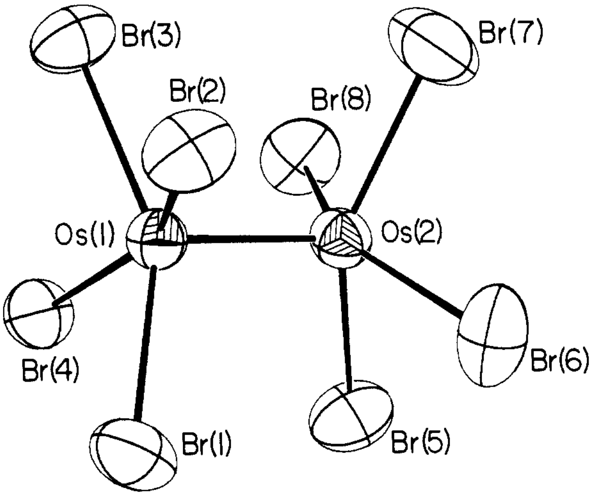

Figure 1. An ORTEP drawing of the $Os_2Br_8^{2-}$ ion, with atoms represented by their 50% probability ellipsoids. The numbering scheme shown applies also to the $Os_2Cl_8^{2-}$ ion.

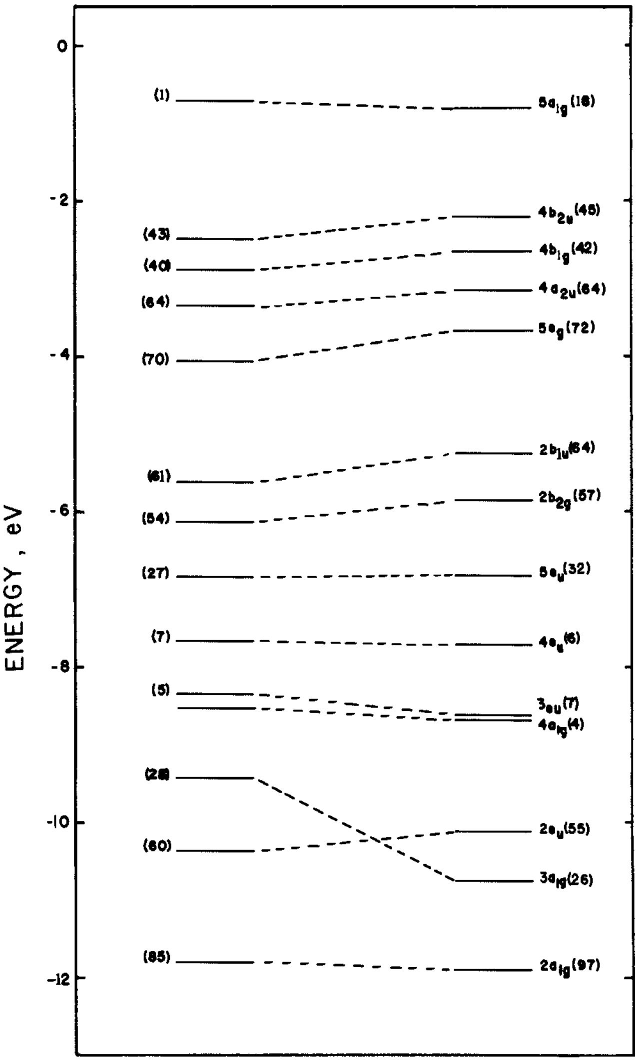

Figure 2. Selected energy levels for the $Os_2Cl_8^{2-}$ ion in an eclipsed (D_{4h}) conformation. The nonrelativistic results are shown at the left and those with relativistic corrections at the right. Figures in parentheses are the % metal orbital contributions.

Structures of the $Os_2X_8^{2-}$ Ions. The atomic positional parameters for the octachloro- and the octabromodiosmate(III) compounds are listed in Tables III and IV. The two compounds are isotypic. While in each case the $Os_2X_8^{2-}$ ion resides on a general position and no crystallographic symmetry is imposed, the symmetry of each $Os_2X_8^{2-}$ ion approximates to D_{4d}, as can be seen by noting the bond distances, bond angles, and torsional angles listed in Table V and by examining the drawing of the $Os_2Br_8^{2-}$ ion shown in Figure 1. The appearance of the $Os_2Cl_8^{2-}$ ion, of which an ORTEP drawing is available in the supplementary material, is virtually identical.

In each case the eight crystallographically independent Os–X distances lie within rather narrow ranges, viz., 2.290 (3)–2.345 (2) Å for Os–Cl, and 2.425 (2)–2.462 (1) Å for Os–Br. The average values, 2.322 [6] and 2.444 [4] Å, respectively, differ by 0.122 [7] Å, which may be compared with the conventional difference of 0.15 Å between the covalent radii of Cl and Br.

The average values of the Os–Os–Cl and Os–Os–Br angles are 104.2 (3)° and 104.3 (4)°, respectively. This is right in the center of the range of such angles in previously studied $M_2X_8^{n-}$ species. Local square pyramidal symmetry within each OsX_4 moiety is closely approximated. The overall molecular symmetry deviates only slightly in each case from D_{4d}, for which the torsion angles would have to be exactly 45°. In the $Os_2Cl_8^{2-}$ ion the mean torsion angle is 49.0 [3]° while in the $Os_2Br_8^{2-}$ ion it is 46.7 [1]°.

SCF-Xα-SW Calculation. The results of the relativistic calculation are presented in Table VI. Figure 2 is an energy level diagram that shows a selected set of molecular orbitals in both the relativistic and the nonrelativistic calculations. Those selected are all of the a_{1g} orbitals, all of the e_u levels, the $\delta(b_{2g})$ and $\delta^*(b_{1u})$ levels, and the lower five empty orbitals. It can be seen that with only one exception ($3a_{1g}$) the inclusion of the relativistic corrections has no major effect. A few comments are now in order about the character of the orbitals.

The $5a_{1g}$ orbital is essentially a Rydberg orbital, mainly concentrated outside of the molecular sphere. The $4b_{2u}$ and $4b_{1g}$ orbitals are Os–Cl antibonding orbitals. The $4a_{2u}$ and $5e_g$ orbitals

Table VI. Upper Valence Molecular Orbitals for Eclipsed (D_{4h}) $Os_2Cl_8^{2-}$ with Relativistic Corrections

level	energy, eV	Os	Cl	Int.[a]	Out.[a]	breadkdown of Os contributions, %			
$5a_{1g}$	−0.808	18	20	18	45	60s	15p	24d	1f
$4b_{2u}$	−2.231	45	46	2	7	100d			
$4b_{1g}$	−2.650	42	47	4	7	99d	1f		
$4a_{2u}$	−3.156	64	20	14	2	9p	89d	2f	
$5e_g$	−3.672	72	21	6	1	98d	2f		
$2b_{1u}$	−5.282	64	26	8	1	100d			
$2b_{2g}$	−5.853	57	30	11	2	100d			
$1a_{1u}$	−6.742	0	90	8	1				
$5e_u$	−6.821	32	55	12	2	10p	88d	2f	
$3b_{2u}$	−6.832	0	90	8	1				
$1a_{2g}$	−6.936	0	88	10	2				
$4e_g$	−7.241	4	85	8	3				
$3e_g$	−7.346	3	85	10	2				
$3a_{2u}$	−7.677	6	77	15	2				
$4e_u$	−7.677	6	80	12	3				
$3b_{1g}$	−7.961	1	84	14	2				
$3e_u$	−8.604	7	80	11	3				
$4a_{1g}$	−8.670	4	75	19	2				
$2e_g$	−8.904	18	74	6	2	28p	71d	1f	
$1b_{1u}$	−9.324	24	61	14	1	99d	1f		
$1b_{2g}$	−9.831	28	54	17	1	100d			
$2e_u$	−10.157	55	36	9	0	99d	1f		
$2a_{2u}$	−10.309	25	73	0	2	56s	2p	41d	1f
$2b_{2u}$	−10.368	39	59	0	2	99d	1f		
$3a_{1g}$	−10.739	26	68	4	2	96s	1p	2d	2f
$2b_{1g}$	−10.823	41	57	0	2	100d			
$2a_{1g}$	−11.886	97	3	0	0	10s	7p	80d	4f

[a] Int. and Out. refer to the percent contributions from the intersphere region and from outside of the outer sphere, respectively.

can be described as the Os–Os σ^* and π^* orbitals.

The $2b_{1u}$ and $2b_{2g}$ orbitals are the δ^* and δ orbitals, respectively, and both are occupied.

There are four orbitals, $2e_u$ to $5e_u$, that have the proper symmetry to participate in Os–Os π bonding, but of these, $2e_u$ is the only one to make a major contribution, with $5e_u$ making a minor one. The $3e_u$ and $4e_u$ orbitals are essentially lone-pair orbitals made up of Cl pπ contributions. The Os–Os σ bonding is carried almost entirely by the $2a_{1g}$ orbital, with the $3a_{1g}$ and $4a_{1g}$ orbitals being mainly concentrated on the Cl atoms.

Discussion

Since the first report[14] of a compound containing an Os^{III}–Os^{III} triple bond, in 1980, there has been steady growth in our knowledge of the chemistry of the Os_2^{6+} complexes.[4b] However, until the discovery of the $Os_2X_8^{2-}$ ions, all of these diosmium compounds have contained bridging bidentate ligands, usually four, though a few have contained only two, viz., the $Os_2(O_2CMe)_2R_4$ (R = CH_2SiMe_3, CH_2CMe_3) compounds mentioned but not otherwise described by Wilkinson et al.,[15] and two compounds[16] containing the $Os_2Cl_4(chp)_2$ unit (chp = anion of 6-chloro-2-hydroxypyridine). The $Os_2Cl_4(chp)_2$ molecule can be considered formally as a substitution derivative of the $Os_2Cl_8^{2-}$ ion, but this is at present a purely formal view since it has not yet been obtained by the reaction of Hchp or chp^- with $Os_2Cl_8^{2-}$. Actually, each of the two compounds containing $Os_2Cl_4(chp)_2$ contains a fairly strongly bound axial ligand (pyridine or H_2O), and the presence of these axial ligands appears to cause a considerable lengthening of the Os≡Os bond, to 2.322 (1) and 2.293 (1) Å, respectively.

Structural Considerations. With regard to the crystal structures of the $(n\text{-}Bu_4N)_2[Os_2X_8]$ compounds, it is to be noted that there is no indication of the type of disorder that is characteristic, and occurs almost without exception, in $M_2X_8^{n-}$ compounds and many of their derivatives, wherein some of the M_2 units lie in one (or even, as in $Re_2Cl_4(PEt_3)_4$, in both) of the directions perpendicular to the main M_2 orientation. This type of disorder comes about most naturally when the M_2X_8 conformation is eclipsed, since the X_8 group then defines a square parallepiped that is practically a cube. As the conformation is twisted away from the eclipsed structure, the occurrence of such a disorder becomes less probable, although in various $M_2X_4(dppe)_2$ compounds (M = Mo, W and X = Cl, Br) it has been observed.[4a] In the $(PPN)_2[Os_2Cl_8]$ structure, where the torsion angle is only about 14°, there is considerable disorder (ca. 36%), but in the compounds studied here, where the torsion angles are close to 45°, no disorder is seen.

Table VII. Correlation Table for an $M_2X_8^{n-}$ Molecule for Conformations with D_{4h}, D_4, and D_{4d} Symmetry

D_{4h}	D_4	D_{4d}
$A_{1g}(\sigma)$ A_{1u}	$A_1(\sigma)$	$A_1(\sigma)$ B_1
A_{2g} $A_{2u}(\sigma^*)$	$A_2(\sigma^*)$	A_2 B_2
B_{1g} $B_{1u}(\delta^*)$	$B_1(\delta^*)$	$E_2(\delta)$
$B_{2g}(\delta)$ B_{2u}	$B_2(\delta)$	
$E_g(\pi^*)$ $E_u(\pi)$	$E(\pi,\pi^*)$	$E_1(\pi)$ $E_3(\pi^*)$

The occurrence of nearly perfect D_{4d} symmetry in the anions of both of the $(n\text{-}Bu_4N)_2[Os_2X_8]$ compounds is in accord with the idea, to be discussed more fully below, that there is a $\sigma^2\pi^4\delta^2\delta^{*2}$ configuration in the ground state of the eclipsed form. From this point of departure one does not anticipate any inherent electronic barrier to rotation. Then, assuming that the interactions between vicinal Os–X bonds are repulsive, a completely staggered structure with D_{4d} symmetry would be expected. It is very likely, however, that the purely nonbonded forces do not give rise to a very large difference in energy between the staggered and eclipsed conformations, especially for the $Os_2Cl_8^{2-}$ ion. Therefore, intermolecular forces (crystal packing) will also play an important role in determining the exact rotational conformation in the crystal. The small deviations from 45° found in these two $(n\text{-}Bu_4N)_2[Os_2X_8]$ compounds are thus not at all surprising. The fact that the $(PPN)_2[Os_2Cl_8]$ compound shows a rotational conformation closer to eclipsed than staggered seems also to be understandable on the basis that the internal steric forces are small enough to have been overwhelmed by the intermolecular forces in that particular crystal.

Bonding Considerations. From a qualitative point of view, one would expect the $Os_2X_8^{2-}$ ions to have five electron pairs available for metal metal bonding and hence in the eclipsed conformation a $\sigma^2\pi^4\delta^2\delta^{*2}$ configuration. An SCF–Xα–SW calculation shows this to be correct, just as in the case of the $Re_2Cl_4(PR_3)_4$ compounds.[17] For the latter, the computational results, including the actual magnitude of the δ–δ^* separation, have recently been corroborated by a measurement of the valence shell photoelectron spectrum of $Re_2Cl_4(PMe_3)_4$.[18]

It is noteworthy that in the other major classes of diosmium(III,III) compounds (see Table 4-1 of ref 4b) there tends to be a near degeneracy of the δ^* and π^* orbitals which leads to temperature-dependent magnetic moments. That is not expected to be the case here since the calculation predicts a separation between the $\delta^*(2b_{1u})$ orbital and the $\pi^*(5e_g)$ orbital of about 1.5 eV.

The eclipsed conformations found in $M_2X_8^{n-}$ species with $\sigma^2\pi^4\delta^2$ and $\sigma^2\pi^4\delta^2\delta^*$ configurations are attributable to the fact that δ-bonding is maximized in the eclipsed conformations. It is clear, therefore, that for a compound with a $\sigma^2\pi^4\delta^2\delta^{*2}$ configuration, rotation toward a completely staggered conformation is not inhibited by the M–M bonding. Thus, since we have found a $\sigma^2\pi^4\delta^2\delta^{*2}$ configuration for $Os_2Cl_8^{2-}$ in the eclipsed (D_{4h}) conformation, we have a theoretical basis for understanding the observed conformations, which are essentially staggered (D_{4d}).

---

[14] Cotton, F. A.; Thompson, J. L. *J. Am. Chem. Soc.* **1980**, *102*, 6437.

[15] Tooze, R. P.; Motevalli, M.; Hursthouse, M. B.; Wilkinson, G. *J. Chem. Soc., Chem. Commun.* **1984**, 799.

[16] Cotton, F. A.; Dunbar, K. R.; Matusz, M. *Inorg. Chem.* **1986**, *25*, 1585, 1589.

[17] Bursten, B. E.; Cotton, F. A.; Fanwick, P. E.; Stanley, G. G.; Walton, R. A. *J. Am. Chem. Soc.* **1983**, *105*, 2606.

[18] Root, D. R.; Blevins, C. H.; Lichtenberger, D. L.; Sattelberger, A. P.; Walton, R. A. *J. Am. Chem. Soc.* **1986**, *108*, 953.

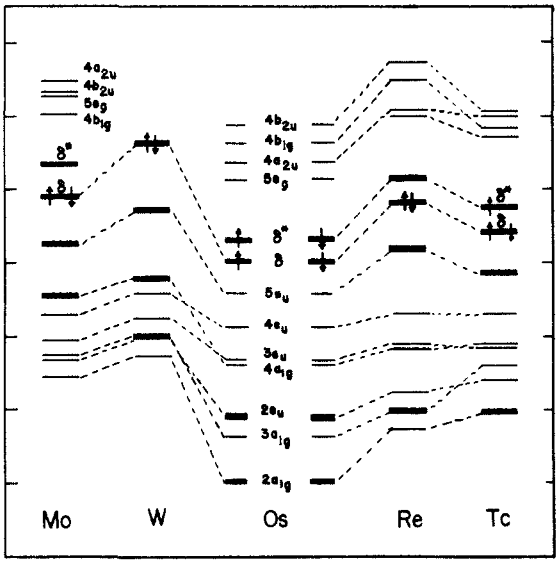

Figure 3. Selected energy levels for the $M_2Cl_8^{n-}$ species that have been treated by the SCF–Xα–SW method. The levels represented by thick lines are those with high (>50%) metal character.

In proceeding from an eclipsed (D_{4h}) to a staggered (D_{4d}) conformation for an $M_2X_8^{n-}$ species, all intermediate conformations are of lower symmetry, viz., D_4. However, the essential symmetry characteristics of the σ, σ^*, π, π^*, δ, and δ^* M–M orbitals can be traced through as shown in Table VII.

It is easiest to recognize and appreciate the relationships between the symmetry types (representations in the character table) and the orbital types based on nodal properties (σ, σ^*, π, etc.) for the eclipsed conformation, D_{4h}. In the exactly staggered conformation, the δ and δ^* orbitals cease to exist as separate types. Instead, the two atomic orbitals which give rise to the energetically separated δ and δ^* combinations in D_{4h} as well as D_4 symmetry afford a basis for the doubly degenerate E_2 representation in D_{4d} symmetry. In effect, as the conformation changes from D_{4h} to D_{4d}, the $\delta^*(b_1)$ and $\delta(b_2)$ orbitals come closer and closer together in energy until they become rigorously degenerate and constitute a doubly degenerate, nonbonding orbital of E_2 symmetry when the rigorously staggered conformation is reached. The $\delta^2\delta^{*2}$ configuration in D_{4h} symmetry becomes an e_2^4 configuration in D_{4d} symmetry. However, there is still a set of σ and π orbitals that can be taken as the basis of a $\sigma^2\pi^4$ net triple bond.

The calculations on the $Os_2Cl_8^{2-}$ ion suggest at least a few assignments of the bands in the visible spectrum. The two bands previously reported[1] for a CH_2Cl_2 solution of $(PPN)_2Os_2Cl_8$, at ca. 13 000 and 21 500 cm^{-1}, with extinction coefficients of 180 and 130, respectively, have been verified with use of a CH_2Cl_2 solution of $(n\text{-}Bu_4N)_2Os_2Cl_8$. In addition, more intense bands ($\epsilon \approx 10000$) have been recorded at ca. 32 000 and 38 500 cm^{-1}. We have not attempted to calculate state energy differences using the transition-state theory, but it is likely that simple orbital energy differences will be fairly reliable for the types of transition we are dealing with since large correlation energies are not to be expected. On this basis, and assuming that the D_{4d} conformation prevails in solution, we can suggest the following tentative assignments.

We suggest assigning the lowest energy band, at ca. 13 000 cm^{-1}, to the $e_2(\delta) \rightarrow e_3(\pi^*)$ transition, which is predicted to be the lowest energy transition at ca. 15 000 cm^{-1} (where we use the difference between the energy of the $5e_g$ and the average energy of the $2b_{1u}$ and $2b_{2g}$ orbitals). Similarly, the orbital energy difference for the $5e_u$ and $5e_g$ orbitals (an $e_1 \rightarrow e_3$ transition in D_{4d}) is ca. 24 000 cm^{-1}, in reasonable agreement with the observed energy (21 500 cm^{-1}) of the next observed band. This transition has both $\pi \rightarrow \pi^*$ and charge-transfer character. Both of these transitions would be dipole-allowed. The next two orbital energy differences (for $4e_u$ and $3e_u$ to $5e_g$) are ca. 32 000 and 39 000 cm^{-1}, which again agree well with the next two observed bands. These two transitions would be virtually pure ligand to metal charge transfer, for which extinction coefficients of about 10 000 are not unreasonable. Of course, only a more detailed spectrosopic study will show whether these assignments are really correct, but the agreement is encouraging.

We turn now to one final topic, and that is a comparison of the present results from the SCF–Xα–SW calculations with those previously obtained for other $M_2Cl_8^{n-}$ ions, namely for $Mo_2Cl_8^{4-}$,[19] $W_2Cl_8^{4-}$,[20] $Re_2Cl_8^{2-}$,[12] and $Tc_2Cl_8^{3-}$.[20] These results, for selected orbitals, are shown and compared with the present ones in Figure 3. It should be noted first that while the overall up and down shifts of the entire sets of orbitals are probably correct qualitatively, they should not be accorded quantitative significance because they are somewhat influenced by the choices of sphere radii, especially that of the Watson sphere used to suppress the influence of the net charge. The features that are of interest are the relative energies of the main δ^*, δ, π, and σ orbitals in each case.

It will be noted that the δ/δ^* separation changes very little from case to case. Moreover, the role of the $5e_u$ orbital as the major contributor (or at least *a* major contributor) to the metal–metal π bonding as well as its position at 1.1 ± 0.2 eV below the δ orbital is a consistent feature of all the results. In the Re, Os, and Tc cases, the $2e_u$ orbital also contributes to M–M π bonding. In all cases, the $4e_u$ and $3e_u$ orbitals have only slight metal d orbital character (2–8%) and are essentially chlorine lone-pair orbitals. The π^* orbital, the $5e_g$ orbital in all cases, lies consistently 1.5–2.0 eV above the δ^* orbital. In view of the consistency of these features from one $M_2X_8^{n-}$ species to another, we believe that the existence of stable, diamagnetic $Ru_2X_8^{2-}$ ions with $\sigma^2\pi^4\delta^2\delta^{*2}$ configurations is highly likely. Efforts to isolate them are in progress.

The a_{1g} orbital that makes the main contribution to metal–metal σ bonding varies somewhat through the series of $M_2X_8^{n-}$ species shown in Figure 3. In the Mo and W compounds, where the metal atoms are formally in the +2 oxidation state, it is the $4a_{1g}$ orbital, but for the other three it is the lower lying $2a_{1g}$ orbital (Os, Tc) or the $3a_{1g}$ orbital (Re). It is not clear whether these variations are of real significance or whether they are somewhat artifactual.

Acknowledgment. We thank the National Science Foundation (Grant No. CHE-8506702 to R.A.W. and Grant No. CHE-8211407 to F.A.C.) and the donors of the Petroleum Research Fund, administered by the American Chemical Society, through a grant to R.A.W., for support of this research.

Registry No. 1, 97523-37-0; **2**, 97523-38-1; $Os_2(O_2CCH_3)_4Cl_2$, 81519-41-7; Os, 7440-04-2.

Supplementary Material Available: Tables of observed and calculated structure factors for both compounds, complete tables of bond lengths and angles, anisotropic displacement parameters, and an ORTEP drawing of the $Os_2Cl_8^{2-}$ ion (59 pages). Ordering information is given on any current masthead page.

---

(19) Norman, J. G., Jr.; Kolari, H. J. *J. Am. Chem. Soc.* **1975**, *97*, 33.
(20) Cotton, F. A.; Kalbacher, B. J. *Inorg. Chem.* **1977**, *16*, 2386.